

ELIMINATING LABEL LEAKAGE IN TREE-BASED VERTICAL FEDERATED LEARNING

A PREPRINT

Hideaki Takahashi*

Jingjing Liu†

Yang Liu‡

July 21, 2023

ABSTRACT

Vertical federated learning (VFL) enables multiple parties with disjoint features of a common user set to train a machine learning model without sharing their private data. Tree-based models have become prevalent in VFL due to their interpretability and efficiency. However, the vulnerability of tree-based VFL has not been sufficiently investigated. In this study, we first introduce a novel label inference attack, **ID2Graph**, which utilizes the sets of record-IDs assigned to each node (i.e., instance space) to deduce private training labels. The ID2Graph attack generates a graph structure from training samples, extracts *communities* from the graph, and clusters the local dataset using community information. To counteract label leakage from the instance space, we propose an effective defense mechanism, **ID-LMID**, which prevents label leakage by focusing on mutual information regularization. Comprehensive experiments conducted on various datasets reveal that the ID2Graph attack presents significant risks to tree-based models such as Random Forest and XGBoost. Further evaluations on these benchmarks demonstrate that ID-LMID effectively mitigates label leakage in such instances.

Keywords Privacy Preserving Machine Learning · Vertical Federated Learning · Label Leakage

1 Introduction

Tree-based models, including a single decision tree and tree ensembles such as random forests (RFs) and gradient boosted decision trees (GBDTs), are among the most widely utilized machine learning algorithms in practice [Kaggle, 2021]. These models work by recursively partitioning the feature space and training a decision tree to make predictions based on these partitions. When training a decision tree, each internal node splits the *instance space*, which is the set of training sample IDs assigned to this node, according to a certain discrete function of the input attributes. Due to growing privacy concerns, tree-based vertical federated learning (T-VFL) [Cheng et al., 2021, Wu et al., 2020, Yin et al., 2021] has grown in popularity [Cheng et al., 2021, Wu et al., 2020, Yin et al., 2021]. T-VFL enables multiple parties with disjoint features of a common user set to train a global tree model collaboratively [Liu et al., 2022a] without exposing their original data. One example is a medical diagnosis model trained on datasets from several hospitals, in which case each hospital may possess a different set of features extracted from the same patient [Liu et al., 2019]. Another example is financial companies who prefer to utilize each other’s private features to create a credit scoring model [Yang et al., 2019, Zheng et al., 2020].

In a typical VFL scheme, only one party, referred to as the active party, has training labels, whereas all the other parties are referred as passive parties. All parties keep their data and models local while utilizing homomorphic encryption, multi-party computation, or both to protect exchanged gradient-related information during training [Yang et al., 2023]. However, recent research show that such VFL algorithms may be still susceptible to label leakage attacks, where a

*The University of Tokyo (this work was done during the internship at Institute for AI Industry Research, Tsinghua University), takahashi-hideaki567@g.ecc.u-tokyo.ac.jp

†Institute for AI Industry Research, Tsinghua University, jjliu@air.tsinghua.edu.cn

‡Corresponding Author, Institute for AI Industry Research, Tsinghua University, Shanghai Artificial Intelligence Laboratory, liuy03@air.tsinghua.edu.cn

passive party attempts to infer labels from the active party using its local results [Fu et al., 2022, Sun et al., 2022, Li et al., 2021]. Despite the fact that tree-based models are deployed more widely than neural networks in practical applications [Kaggle, 2021], most existing research on VFL focuses on the latter, and the potential vulnerability of tree-based models has not been well studied. In a Tree-based VFL scheme, instance space of each node is also communicated for split finding [Cheng et al., 2021]. Although Cheng et al. [2021] suggests that a passive party might be able to infer training labels from the exposed instance space, it is unclear how and to what extent the attacker can steal training labels. This concern has not been widely recognized, as many recent works [Cheng et al., 2021, Suthampan and Maneewongvatana, 2005, Liu et al., 2020, Hou et al., 2021, Fu et al., 2021, Chen et al., 2021, Xu et al., 2023, Liu et al., 2022b, Yao et al., 2022, Tian et al., 2020, Zhu et al., 2021, Wang et al., 2022] still reveal the instance space to all parties.

In this study, we propose a novel **ID2Graph** attack, which allows an honest-but-curious passive party to infer private training labels from instance space exposed with high accuracy. We execute the attack by extracting a graph structure from data records used to train the tree-based model, then applying community detection to cluster the learned graph. To eliminate such leakage risk, we propose **ID-LMID**, an effective mutual-information-based defense mechanism that successfully prevents label leakage without sacrificing the utility of the trained model. Our contributions are two-fold: 1) we propose a novel label inference attack against tree-based vertical federated learning, and demonstrate its effectiveness through comprehensive experiments; 2) we present a scalable defense algorithm and showcase its superiority to existing defense mechanisms.

2 Tree-based Vertical Federated Learning

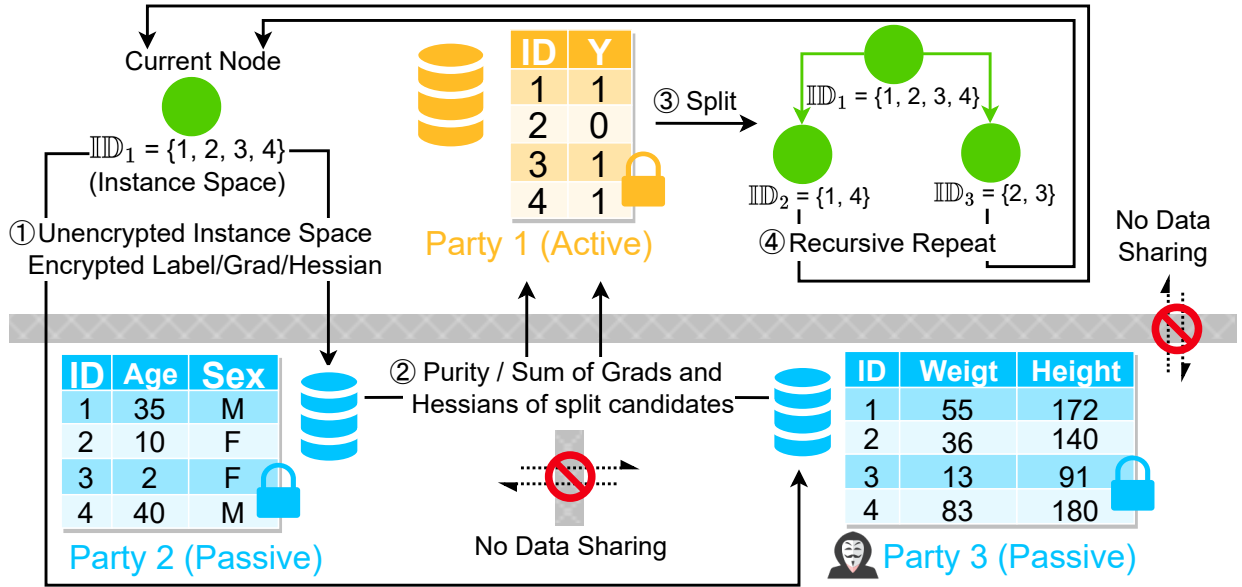


Figure 1: Overview of a tree-based VFL framework where three parties collaboratively train a tree-based model by securely evaluating each split candidate. Since the active party shares the instance space of a node for further split, one malicious passive party might be able to steal ground-truth label information from the instance space the active party shared with him.

To formulate the problem, we assume the entire dataset has N records, and each of M parties has a subset of disjoint features. We denote the set of local datasets as $\{\mathbf{X}^m \in \mathbb{R}^{N \times |\mathbb{F}_m|}\}_{m=1}^M$, where \mathbb{F}_m is the set of local features of the m -th party, and $|\mathbb{F}_m|$ is the number of features of the m -th party. $\forall m \neq m' \in \{1, \dots, M\}$, $\mathbb{F}_m \cap \mathbb{F}_{m'} = \emptyset$. We focus on classification tasks with $|\mathbb{C}|$ classes, where \mathbb{C} is the set of classes, and only the active party, has the ground-truth labels $\mathbf{y} \in \mathbb{R}^N$. Let \mathcal{P}_m be the m -th party, and we assume that \mathcal{P}_1 is the active party, and the others are passive parties.

Tree-based methods learn a model by recursively splitting the instance space of the current node into several subspaces with certain criteria. For example, Random Forest determines the best split with purity-based gain for the classification task from the set of sub-sampled features. One of the popular metrics is Gini-gain defined as $\frac{n^L}{n} \sum_{c \in \mathbb{C}} (\frac{n^{L,c}}{n^L})^2 + \frac{n^R}{n} \sum_{c \in \mathbb{C}} (\frac{n^{R,c}}{n^R})^2 - \sum_{c \in \mathbb{C}} (\frac{n^c}{n})^2$, where n , n^L and n^R are the number of samples assigned to the parent, left child,

and right child node, respectively. $n^{L,c}$ and $n^{R,c}$ are the numbers of data points with class c within the left and right nodes. XGBoost [Chen and Guestrin, 2016] chooses the best split threshold that maximizes the following gain: $\frac{1}{2}[\frac{(g^L)^2}{h^L+\lambda} + \frac{(g^R)^2}{h^R+\lambda} - \frac{g^2}{h+\lambda}] - \gamma$, where g and h are the sums of gradients and Hessians within the current node, and g^L , g^R , h^L , and h^R are those of left and right child nodes after the split, respectively. λ and γ are hyper-parameters. The instance space \mathbb{ID}_u^t is defined as the assignment of data samples IDs to the u -th node of the t -th tree. A node is called a leaf when it does not have any children.

Following prior work [Cheng et al., 2021, Liu et al., 2020, Fu et al., 2021, Chen et al., 2021, Xu et al., 2023, Liu et al., 2022b, Yao et al., 2022, Zhu et al., 2021, Wang et al., 2022], active and passive parties train $|\mathbb{T}|$ trees in total (\mathbb{T} denotes the set of trees) by communicating necessary secure statistics to find the best split as well as plain-text instance space for each split. Specifically, Secureboost [Cheng et al., 2021] repeatedly communicates encrypted gradients and Hessian in XGBoost, as well as instance spaces and split information of the current node, including best-split feature ID and threshold ID. Similarly, Vertically Federated Random Forest [Yao et al., 2022] repeatedly communicates ciphered purity score, as well as instance spaces and split information of the current node. See Figure 1 for the overview of a T-VFL framework and Appendix A for their pseudo-codes.

3 ID2Graph Attack

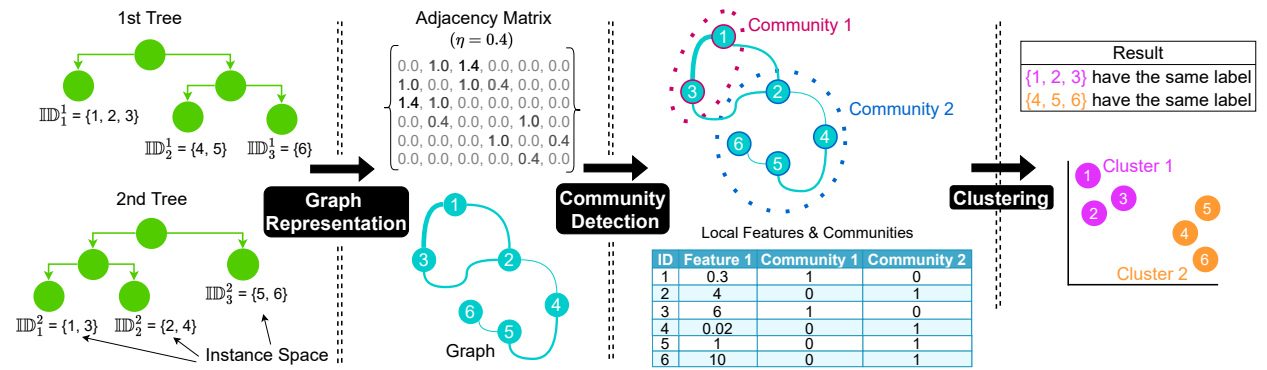


Figure 2: Illustration of ID2Graph. This method consists of 1) creating a graph of data points from the trained model, 2) grouping the vertices of the graph to communities, and 3) clustering the local dataset along with extracted communities to estimate which data samples belong to the same label.

Our proposed attack, ID2Graph, is an attack that a passive party uses to infer training labels y from the instance space exposed to him during T-VFL training.

Threat Model. Based on T-VFL algorithms above, we consider the honest-but-curious threat model. Specifically, all parties adhere to the given protocol, do not possess auxiliary information nor engage in side-channel attacks such as analyzing timing, power consumption, or network traffic. The attack controls one passive party \mathcal{P}_m where it has access to the local data X^m and instance spaces sent to him from the active party $\mathbb{ID}_m = \{\mathbb{ID}_u^t\}_{(t,u) \in \mathcal{P}_m}$, and the number of classes $|C|$. Each party also knows the threshold values only for nodes whose threshold feature is owned by that party. Given the above information, the attacker attempts to infer which training data points belong to the same class.

To extract intrinsic patterns of training samples, our ID2Graph attack consists of three stages (See Fig. 2): 1) *Graph Representation*: converting the trained model to a graph of record ids; 2) *Community Detection*: abstracting communities within the graph; 3) *Clustering*: clustering the dataset with assigned communities.

Graph Representation As suggested in Cheng et al. [2021], it is natural to assume that data instances assigned to the same leaf of the trained model share similarities. Thus, we use a graph structure to represent the relationships across training samples. Each vertex of the graph represents a corresponding data point, and two vertices are connected if they belong to the same leaf (we use *vertex* for graph and *node* for tree). Specifically, we convert a trained ensemble tree model to an adjacency matrix $A \in \mathbb{R}^{N \times N}$, as follows:

$$A_{i,i'} = \sum_{t=1}^{|\mathbb{T}^m|} \sum_{u=1}^{U_t} \eta^{t-1} \mathbb{1}_{\mathbb{ID}_u^t}(x_i) \mathbb{1}_{\mathbb{ID}_u^t}(x_{i'}) \mathbb{1}_{\text{leaf}^t}(u) \quad (1)$$

, where $|\mathbb{T}^m|$ is the number of trees available to the passive party m ; U_t is the number of nodes of the t -th available tree from the viewpoint of the attacker; leaf^t is the set of leaves within the t -th tree; and η is the discount weight of each tree. $\mathbb{1}$ is the indicator function where $\mathbb{1}_S(x) = 1$ if $x \in S$, else 0. Note that the leaves the attacker possesses are not the same as ground-truth leaves of the model because the attacker can obtain the instance space of leaf nodes only if it possesses the attribute that splits the node. Our approach only relies on \mathbb{T}^m and not on \mathbb{T} .

Since storing the adjacency matrix A requires a space complexity of $O(N^2)$ in the worst case, even with the use of a sparse matrix, we adopt an approximate representation for large datasets that reduces the necessary memory to $O(BN)$, where B is an arbitrary integer. To achieve this, we divide the instance space into multiple chunks of length B . We use the same intra-chunk edges within each chunk as in Eq. 1. We also add a few inter-chunk edges to maintain the binding relationship across the instance space. This process makes A more sparse, decreasing the amount of required memory. Further details can be found in the Appendix B.

Community Detection The traditional community detection method is a popular tool to cluster vertices of a graph into multiple communities, where vertices in each community are tightly linked, and vertices in different communities are loosely connected. We adopt Louvain method [Blondel et al., 2008], one of the fastest algorithms for community detection, which extracts communities by optimizing modularity Q (a metric of community quality) as follows:

$$Q = (1/(2 \sum_{v,v'} A_{v,v'})) \sum_{v,v'} [A_{v,v'} - (\sum_{v'} A_{v,v'} \sum_v A_{v,v'}) / (2 \sum_v \sum_{v'} A_{v,v'})] \delta(\pi_v, \pi_{v'}) \quad (2)$$

, where π_v is the community assigned to the v -th vertex, and δ is the Kronecker delta function, i.e., $\delta(\pi_v, \pi_{v'})$ is one when $\pi_v = \pi_{v'}$ and zero otherwise. Higher Q indicates denser connections within a community and looser links between different communities. After initially assigning each vertex to its own community, Louvain method iteratively executes modularity optimization and community aggregation to maximize Q . During the modularity optimization phase, Louvain method moves each vertex to the best neighboring community, which improves Q until saturation. Then, Louvain method generates a new graph whose vertices represent communities detected during the previous optimization phase. The pseudo-code and implementation details can be found in Appendix C.

Clustering After partitioning the training dataset to the best communities, the attacker utilizes allocations of communities as features for clustering. In this study, we adopt K-means [Hartigan and Wong, 1979, Ahmed et al., 2020], to group the dataset to $|\mathbb{K}|$ clusters, where \mathbb{K} represents the set of cluster labels (see Appendix. D for the pseudo code). We apply min-max normalization to local features for pre-processing and convert the assigned communities to dummy variables. Since we assume that the attacker is aware of the number of class categories, the attacker sets the number of clusters $|\mathbb{K}|$ to $|\mathbb{C}|$.

We will show in Experiments that ID2Graph is able to steal label information with much higher success rate than other methods, posing a great threat to T-VFL system.

4 ID-LMID Defense

In order to mitigate the leakage about the labels from the instance space obtained by the passive party, we propose a novel defense mechanism ID-LMID, which prevents label leakage by reducing the mutual information (MI) between label and instance space. Since MI directly measures the amount of label information extractable from the instance space, restricting MI leads to less data leakage. In this section, we first prove we can track the upper bound of mutual information between label and instance space. Then, we build a practical defense algorithm that internally limits the upper bound of mutual information without adding noise to training labels.

Theorem 1. *Let X, Y be the training data and label, respectively, and S_w be the indicator variable for the instance space of the w -th node of a tree model trained with X and Y , that is, $S_w = \mathbb{1}_{\mathbb{D}_w}(X)$, where $\mathbb{1}_{\mathbb{D}_w}$ is the indicator function for \mathbb{D}_w , the instance space of the w -th node. Then, $I(Y; S_w)$, mutual information between Y and S_w , is bounded as follows:*

$$I(Y; S_w) \leq \max(\sum_{c \in \mathbb{C}} \frac{n_w^c}{n_w} \log \frac{n_w^c/n_w}{N^c/N}, \sum_{c \in \mathbb{C}} \frac{\bar{n}_w^c}{\bar{n}_w} \log \frac{\bar{n}_w^c/\bar{n}_w}{N^c/N}) \quad (3)$$

, where N^c is the total number of samples in class c , n_w is the number of samples within the w -th node, n_w^c is the number of samples within the w -th node with class c , $\bar{n}_w = N - n_w$, and $\bar{n}_w^c = N^c - n_w^c$.

In addition, upper bounding $I(Y; S_w)$ leads to the upper bound of $I(Y; S_1, S_2, \dots, S_w, \dots, S_W)$, the mutual information between the label and the set of instance spaces.

Proposition 1. *Let W be the number of instance spaces within the entire tree ensemble. Then, if $\forall w \in \{1, 2, \dots, W\} I(Y; S_w) \leq \xi$, we have $I(Y; S_1, S_2, \dots, S_w, \dots, S_W) \leq W\xi + (W - 1) \log 2$.*

Proofs of this theorem and proposition can be found in Appendix E.

Based on Theorem 1, if the active party aims to control $I(Y; S_w)$ not to exceed an arbitrary value ξ , it can achieve this goal by making any node visible to passive parties satisfy the following condition:

$$\max(\sum_{c \in \mathbb{C}} \frac{n_w^c}{n_w} \log \frac{n_w^c/n_w}{N^c/N}, \sum_{c \in \mathbb{C}} \frac{\bar{n}_w^c}{\bar{n}_w} \log \frac{\bar{n}_w^c/\bar{n}_w}{N^c/N}) \leq \xi \quad (4)$$

We further show that with this threshold set, the passive party is guaranteed not to learn more information with the following corollary.

Corollary 1. *Eq. 4 guarantees that the attacker cannot get more label information than threshold ξ by applying any mechanism \mathcal{M} to the instance space.*

Proof. Based on Theorem 1 and following data processing inequality [Cover, 1999], the output of any mechanism \mathcal{M} that takes S_w cannot increase mutual information:

$$I(Y; \mathcal{M}(S_w)) \leq I(Y; S_w) \leq \xi \quad (5)$$

□

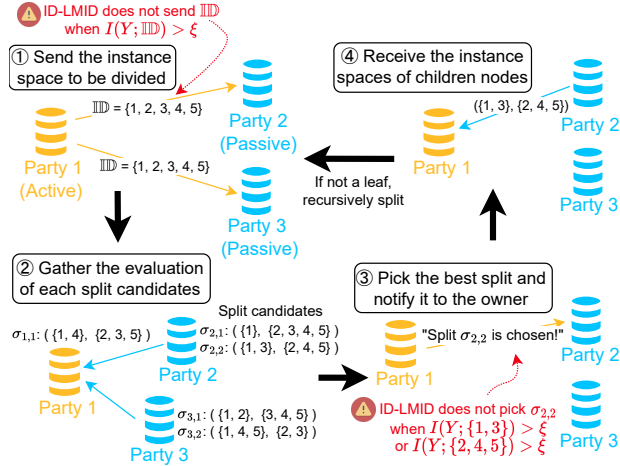


Figure 3: Example of Split Finding within ID-LMID, where ID-LMID identifies potential leakage in instance spaces from both the active and passive sides, and prevents passive parties from accessing the instance spaces that breaks Eq. 4 for all cases.

Algorithm 1 Split Finding with ID-LMID

- 1: \mathcal{P}_1 gathers the evaluation of split candidates $\Gamma = \bigcup_{m=1}^M \Gamma^m$.
- 2: **for** $m \leftarrow 2$ to M **do**
- 3: **for** each split candidate $\sigma_{m,k} \in \Gamma^m$ **do**
- 4: **if** left or right child produced by $\sigma_{m,k}$ does not satisfy Eq. 4 **then**
- 5: $\Gamma^m \leftarrow \Gamma^m \setminus \{\sigma_{m,k}\}$
- 6: \mathcal{P}_1 picks the best split σ_{m^*,k^*} from $\Gamma = \bigcup_{m=1}^M \Gamma^m$.
- 7: **if** left or right child produced by σ_{m^*,k^*} does not satisfy Eq. 4 **then**
- 8: **If not terminated, all children are trained only with the active party \mathcal{P}_1 .**
- 9: **else**
- 10: \mathcal{P}_{m^*} receives k^* and sends the instance spaces of children nodes to \mathcal{P}_1 .
- 11: **If not terminated, the children are recursively trained with all parties.**

As a practical mechanism, we propose ID-Label Mutual Information-based Defense (ID-LMID), which makes all instance spaces visible to passive parties satisfy $I(Y; S_w) \leq \xi$ under Theorem 1. Note that under a T-VFL scheme, we observe that a passive party can obtain the instance space of a node under two conditions: 1) it knows the threshold that produces that node, or 2) directly receives the instance space from the active party. Based on the above observations, ID-LMID introduces two MI constraints to the original T-VFL protocol when finding the best split for each node. Specifically, to avoid leakage under condition 1), the active party does not adopt any split candidate from a passive party that generates a child node violating Eq. 4, which eliminates all of the unsatisfactory split candidates from passive parties. To avoid leakage from condition 2), the active party does not broadcast the instance space when the left or right node of the split breaks Eq. 4, but searches the best split exclusively using its own dataset.

Algo. 1 presents the overview of ID-LMID, where $\sigma_{m,k}$ is k -th split candidate of m -th party, and Γ^m denotes the set of split candidates of m -th party. Line 2 ~ 5 implements the first constraint, and Line 7 ~ 11 corresponds to the second

constraint. Finally, evaluating the first constraint (Line 4 in Algo. 1) requires the active and passive party to calculate node purity (n_w^c/n_w and \bar{n}_w^c/\bar{n}_w) in Eq. 4 in a secure manner without exposing sensitive information to each other, which has been widely studied before using multi-party computation (MPC) [Suthampan and Maneewongvatana, 2005, Liao et al., 2022], homomorphic encryption(HE) [Wu et al., 2020, Liu et al., 2020, Xu et al., 2023, Yao et al., 2022], or without protection [Hou et al., 2021, Liu et al., 2022b]. In this work, we adopt the Homomorphic Encryption(HE)-based implementation [Xu et al., 2023, Yao et al., 2022] and propose our algorithm for evaluating Eq. 4 (See Algo 2). In Algo 2, we use y_i^c to denote the c -th position of the one-hot encoded label y_i , and use $\llbracket \cdot \rrbracket$ to denote a value encrypted with Paillier Encryption [Paillier, 1999], which is popular HE technique that allows the addition between ciphertexts and multiplication between ciphertext and plaintext. Then, node purity of each split candidate can be securely calculated by summing the corresponding encrypted labels. Similar to many existing frameworks [Cheng et al., 2021, Chen et al., 2021, Xu et al., 2023, Yao et al., 2022], this procedure only discloses the aggregated statistics to the active party, and no other information is revealed to any party.

Algorithm 2 Seure Computation of Node Purity with HE

- 1: \mathcal{P}_1 encrypts one-hot encoded label $\{\{y_i^c\}_{c=1}^C\}_{i=1}^N$ with Paillier Encryption and broadcasts $\{\{\llbracket y_i^c \rrbracket\}_{c=1}^C\}_{i=1}^N$ to all passive parties.
 - 2: **for** $m \leftarrow 2 \dots M$ **do**
 - 3: **for** $\sigma_{m,k} \in \mathbb{D}^m$ **do**
 - 4: $\mathbb{D}_L, \mathbb{D}_R \leftarrow$ Instance space of the left and right child nodes divided with $\sigma_{m,k}$
 - 5: $\bar{\mathbb{D}}_L \leftarrow \{1, 2, \dots, N\} \setminus \mathbb{D}_L, \bar{\mathbb{D}}_R \leftarrow \{1, 2, \dots, N\} \setminus \mathbb{D}_R$
 - 6: \mathcal{P}_m sends $\{(1/|\mathbb{D}_L|) \sum_{i \in \mathbb{D}_L} \llbracket y_i^c \rrbracket\}_{c=1}^C$ and $\{(1/|\bar{\mathbb{D}}_L|) \sum_{i \in \bar{\mathbb{D}}_L} \llbracket y_i^c \rrbracket\}_{c=1}^C$ to \mathcal{P}_1
 - 7: \mathcal{P}_m sends $\{(1/|\mathbb{D}_R|) \sum_{i \in \mathbb{D}_R} \llbracket y_i^c \rrbracket\}_{c=1}^C$ and $\{(1/|\bar{\mathbb{D}}_R|) \sum_{i \in \bar{\mathbb{D}}_R} \llbracket y_i^c \rrbracket\}_{c=1}^C$ to \mathcal{P}_1
 - 8: \mathcal{P}_1 decrypts purities submitted by \mathcal{P}_m for both children and evaluates Eq. 4.
-

5 Experiments

5.1 Settings

Datasets and Models We conduct experiments on a two-party VFL system over nine different datasets ranging from hundreds to hundreds of thousands of samples: 1) *Breastcancer* [Dua and Graff, 2017]; 2) *Phishing* [Dua and Graff, 2017]; 3) *Credit* [Dua and Graff, 2017]; 4) *Obesity* [Dua and Graff, 2017, Palechor and de la Hoz Manotas, 2019]; 5) *Nursery* [Dua and Graff, 2017]; 6) *Avila* [Dua and Graff, 2017, De Stefano et al., 2018]; 7) *Drive* [Dua and Graff, 2017]; 8) *Fars* [Olson et al., 2017] and 9) *Purcio* [Dua and Graff, 2017, Ugulino et al., 2012]. The details of these datasets can be found in Appendix H. We utilize 80% of each dataset for training and the remaining 20% of data as the test dataset. All the labels are held by one of two parties, the active party, while the other passive party tries to steal the labels. We vertically and randomly partition features into two halves as the local datasets of the two parties. Note that from the attacker’s perspective, this setting is the same as when the attacker possesses 50% of features and one active and multiple passive parties have the remaining features. We further evaluate the impact of feature partitions using feature importance metrics [Kraskov et al., 2004] on attack results.

We employ Random Forest and XGBoost as the target tree-based methods, with a depth of 6, a feature sub-sampling ratio of 0.8, and a tree size of 5 as the default setting. We use a learning rate of 0.3 for XGBoost and η of 0.6 for XGBoost and 1.0 for Random Forest. Our hyperparameters are consistent with prior works, with the sampling ratio and learning rate from [Cheng et al., 2021], the depth from [Chen and Guestrin, 2016], and the number of trees based on [Wu et al., 2020]. Since our main focus is evaluating potential attack and defense performance rather than achieving high accuracy on the main task of VFL, we did not perform fine-tuning of these hyperparameters.

For evaluation metrics, we use V-measure [Rosenberg and Hirschberg, 2007] to measure how accurately the estimated clusters correspond to ground-truth labels (see Appendix F for detailed definitions). All results are averaged over five different random seeds.

Baselines To evaluate our ID2Graph Attack, we compare with the following baselines: 1) Clustering (CL). We apply k-means clustering to the attacker’s local features as a baseline for label leakage. 2) Union Attack (UNI). UNI is the naive approach in Secureboost [Cheng et al., 2021], where the attacker approximates that arbitrary two samples have the same label if these two samples are assigned together to at least one node. 3) UNI+CL. This method combines UNI and CL by using the result of UNI as additional features for k-means clustering.

To evaluate our ID-LMID defense, we compare it to two existing mechanisms: Reduced-Leakage [Cheng et al., 2021] and LP-MST [Ghazi et al., 2021], which protects labels based on randomized response (see Appendix G for the detail and pseudo code). Since Reduced-Leakage is intended for gradient-boosting, we apply it solely to XGBoost. We employ two stages (LP-2ST) for LP-MST and set its privacy budget ϵ to [0.1, 0.5, 1.0, 2.0]. Finally, we set ξ to [0.05, 0.1, 0.3, 1.0] for ID-LMID.

5.2 Attack Results

Tab. 1 summarizes V-measure scores of different attacks. Results show that ID2Graph attack leads to higher V-measures than clustering on local features only, implying that the proposed attack can steal private label information from the trained model. ID2Graph also outperforms Union Attack, indicating that ID2Graph can extract more label information from the instance space than Union Attack. Union Attack, in some cases, ends up assigning all samples to the same cluster, which renders V-measure zero. The combination of Union Attack and clustering tends to be better than other baselines, but it is still less effective than ID2Graph.

Table 1: Attack results (CL: clustering, UNI: Union Attack). We measure the performance of each attack with V-measure. ID2Graph leads to better grouping than baseline on all metrics and models.

	Random Forest				XGBoost		
Dataset	CL	UNI	UNI + CL	ID2Graph	UNI	UNI + CL	ID2Graph
<i>Breastcancer</i>	0.554	0.000	0.554	0.806	0.000	0.554	0.755
<i>Obesity</i>	0.254	0.001	0.265	0.550	0.000	0.254	0.517
<i>Phishing</i>	0.001	0.196	0.202	0.488	0.196	0.202	0.409
<i>Nursery</i>	0.036	0.090	0.086	0.307	0.088	0.084	0.213
<i>Credit</i>	0.001	0.029	0.03	0.081	0.029	0.030	0.077
<i>Avila</i>	0.085	0.043	0.093	0.246	0.000	0.085	0.175
<i>Drive</i>	0.283	0.135	0.296	0.719	0.000	0.283	0.660
<i>Fars</i>	0.187	0.506	0.453	0.553	0.224	0.308	0.522
<i>Pucrio</i>	0.075	0.238	0.217	0.441	0.159	0.170	0.361

Impact of Feature Partition. Additionally, we study how the quality of attacker’s local features impacts the attack performance. Specifically, we use mutual information [Kraskov et al., 2004] between each feature and label to quantify feature importance and sort features in descending order. Then, we distribute the top k-percentile features to the attacker and assign the remaining features to the active party. Fig. 4 shows the attack results of each method on various percentiles (left y-axis) and feature importance (right y-axis). Note that the left y-axes have different scales for better visibility. ID2Graph surpasses other baselines in most cases, which indicates that the extracted community information stabilizes clustering regardless of the constitution of the local dataset. We also notice that the V-measure does not continuously improve for certain datasets as the number of available features increases since including non-informative or bad features may counteract the label inference performance.

We also investigate the impact of the maximum depth constraints and the number of trees on the attack performance and visualize some results of clustering in Appendix H.

5.3 Defense Results

Fig. 5 and Fig. 6 show the AUC of the trained VFL model on the test dataset (x-axis) and the attack performance (y-axis) with Reduced-Leakage, LP-2ST, and ID-LMID defenses. A defense is considered ideal when its result locates at the bottom right of the figure, indicating high performance on the main VFL task and a lower success rate for the attack. For LP-2ST and ID-LMID, smaller dots indicate a lower privacy budget, leading to more robust defense at the cost of higher utility loss (therefore appearing on the left bottom of the figure). ID-LMID yields a better trade-off between privacy and utility compared to other methods in most settings. This result suggests that ID-LMID can help find well-fitted tree structures that do not excessively utilize the features of passive parties, which prevents the adversary from obtaining enough information to infer the training labels. Further analysis of the impact of feature partitions on ID-LMID defense is provided in Appendix H, which shows that ID-LMID also works better than other methods, even if the active party has no feature.

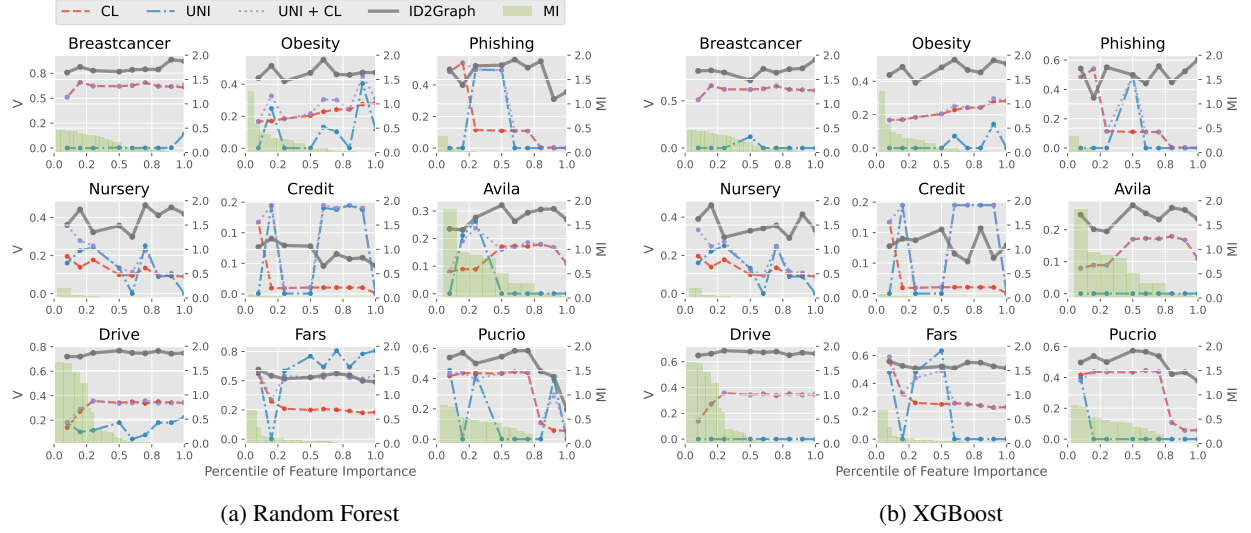


Figure 4: Impact of feature importance on attack performance. ID2Graph outperforms baselines in most cases regardless of the informativeness of the local dataset. X-axis is the top % important features the attacker has. Mutual information scores are represented by bars.

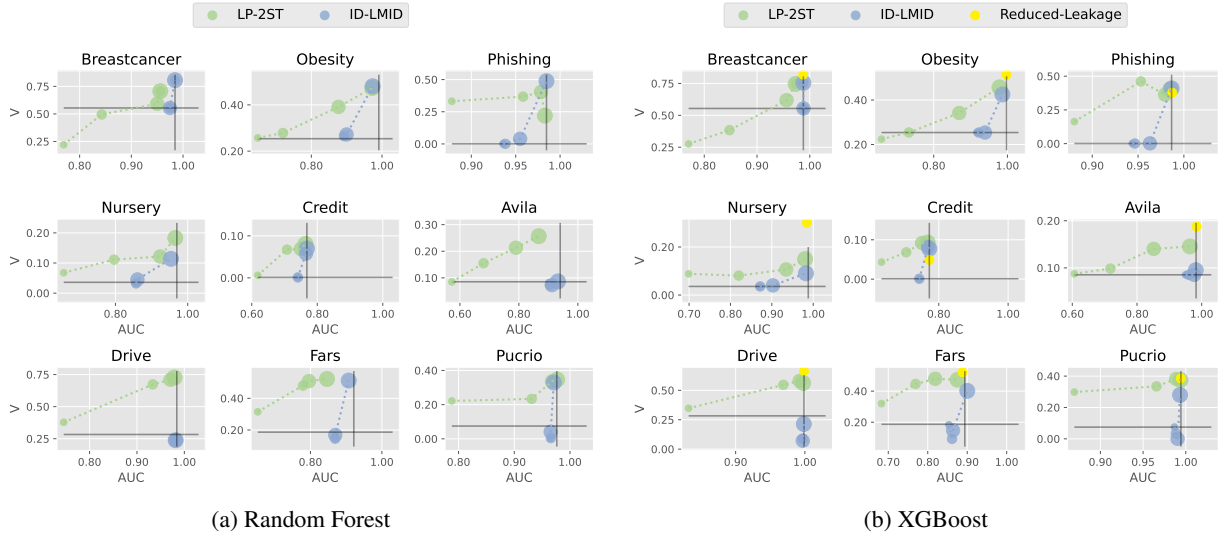


Figure 5: Defense results against ID2Graph attack: the AUC of the trained VFL model on the test dataset (x-axis) and the attack performance of ID2Graph (y-axis) with Reduced-Leakage, LP-2ST, and ID-LMID defenses. The marker size is proportional to the privacy budget: ϵ for LP-MST and ξ for ID-LMID. The horizontal black line is the CL results, and the vertical black line shows AUC of main task without any defense. ID-LMID achieves the best privacy-utility trade-off. We use different scales for x- and y-axes for better viewing.

6 Related Work

Tree-based Vertical FL Federated learning (FL) is a technique that enables training models on decentralized data sources without sharing local raw data. Vertical federated learning (VFL) is one type of FL where each party owns a vertically partitioned dataset. Tree-based Vertical FL (T-VFL) has been actively studied due to its efficiency and practicality. Whereas classic works [Suthampan and Maneewongvatana, 2005, Du and Zhan, 2002, Vaidya et al., 2008, Gangrade and Patel, 2009] mostly focus on securely training a single decision tree on a vertically federated dataset, recent works propose algorithms for privacy-preserving tree ensembles, including bagging [Liu et al., 2020, Hou et al., 2021, Xu et al., 2023, Liu et al., 2022b, Yao et al., 2022] and boosting [Cheng et al., 2021, Fu et al., 2021, Chen et al., 2021, Tian et al., 2020, Zhu et al., 2021, Wang et al., 2022].

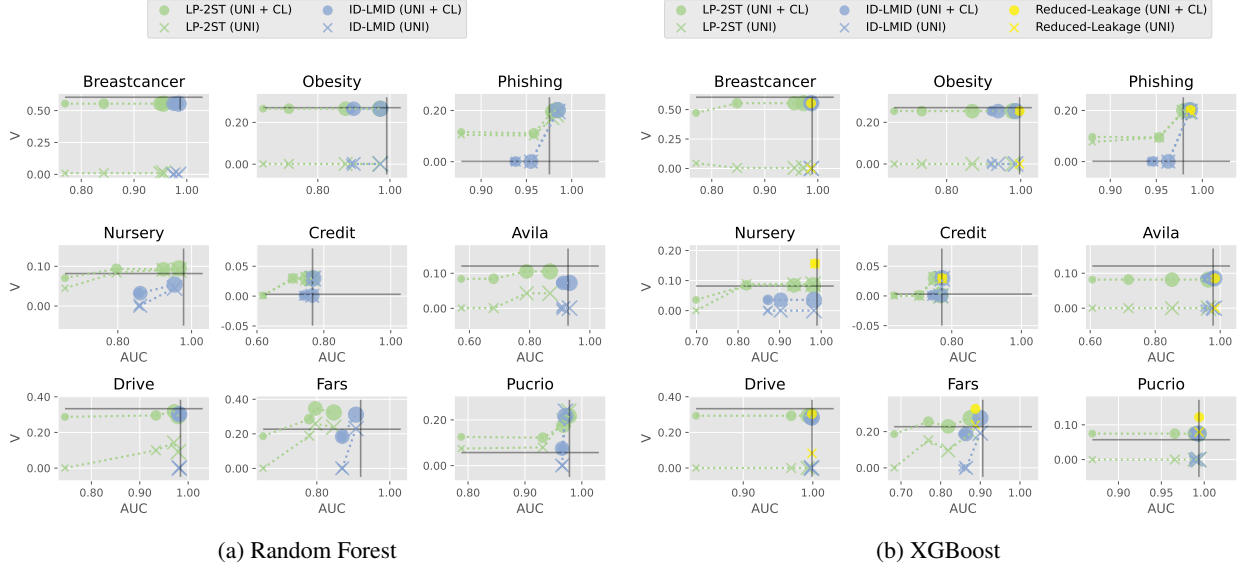


Figure 6: Defense results against Union Attack (UNI) and the combination of UNI and Clustering (UNI + CL). The format is the same as Fig. 5. ID-LMID achieves the best privacy-utility trade-off.

Label Inference Attack in VFL Label inference attack in VFL is typically conducted at a passive party of a VFL system in order to inferring training labels held by the active party [Liu et al., 2022a]. Most existing works only apply to VFL systems trained on logistic regression [Tan et al., 2022] or neural networks [Li et al., 2021, Fu et al., 2022, Sun et al., 2022, Kariyappa and Qureshi, 2021, Qiu et al., 2022, Wainakh et al., 2022, 2021] models, where T-VFL systems are much less studied. For T-VFL, [Wu et al., 2020] suggests that the attacker can infer each sample’s label if each node’s weight is obtainable. However, this is infeasible in many protocols, such as Secureboost where the weight of each node is not exposed to passive parties. [Cheng et al., 2021] finds that the instance spaces, which are not concealed from passive parties in many existing studies [Cheng et al., 2021, Suthampan and Maneewongvatana, 2005, Liu et al., 2020, Hou et al., 2021, Fu et al., 2021, Chen et al., 2021, Xu et al., 2023, Liu et al., 2022b, Yao et al., 2022, Tian et al., 2020, Zhu et al., 2021, Wang et al., 2022], might cause label leakage, yet how accurately the attacker can infer the labels from these instance spaces are not well-studied.

Defense against Label Leakage in VFL Current defense strategies can be broadly categorized into non-cryptographic and cryptographic approaches. Cryptographic approaches protect intermediate information, including the instance space, using Multi-party Computation (MPC) [Hoogh et al., 2014, Adams et al., 2021, Abspoel et al., 2020, Deforth et al., 2021] or Homomorphic Encryption (HE) [Wu et al., 2020, Fang et al., 2021], but the communication and computation costs are too high for realistic situations [Wu et al., 2020, Fang et al., 2021]. Non-cryptographic approaches aim to prevent information leakage by introducing constraints or noise into the training process. Reduced-Leakage for SecureBoost [Cheng et al., 2021] trains the first tree without using passive parties, thus limiting their access to label information. However, this approach relies on the strong assumption that the training dataset is large enough and the model depth is shallow enough. Differential privacy (DP) rigorously quantifies information leakage from statistical algorithms [Dwork et al., 2014, Alvim et al., 2011]. Label DP [Ghazi et al., 2021, Beimel et al., 2013, Chaudhuri and Hsu, 2011] is proposed to tackle the situation where only labels are sensitive information. One DP-based practical algorithm that prevents label leakage from tree-based models is LP-MST [Ghazi et al., 2021]. However, Differential privacy often sacrifices utility to prevent privacy attacks sufficiently [Wang et al., 2021]. Mutual information-based defense can limit the dependency between two variables to prevent the adversary from estimating one variable from the other [Wang et al., 2021, Farokhi and Kaafar, 2020], which applicability on label leakage in T-VFL has not been studied before.

7 Conclusion

This work explores the vulnerability of Tree-based VFL to label inference attacks and demonstrates that instance spaces exchanged in a typical Tree-based VFL system can be exploited to infer sensitive training labels with high accuracy via ID2Graph attack. To counteract label leakage, we propose a mutual information-based defense, ID-LMID.

Experiments on diverse datasets illustrate the significant risk of label leakage from the instance space, as well as the effectiveness of ID-LMID defense compared with other existing solutions. Future work might include better community detection and clustering methods, such as community detection with node attributes, other weighting strategies for adjacency matrix, and tighter upper bound of mutual information between instance space and labels. We hope our study stimulates a re-evaluation of data safety for tree-based VFL schemes and inspires future work on defense strategies for T-VFL.

References

- Kaggle. 2021 kaggle machine learning & data science survey, 2021. URL <https://www.kaggle.com/competitions/kaggle-survey-2021/overview>.
- Kewei Cheng, Tao Fan, Yilun Jin, Yang Liu, Tianjian Chen, Dimitrios Papadopoulos, and Qiang Yang. Secureboost: A lossless federated learning framework. *IEEE Intelligent Systems*, 36(6):87–98, 2021.
- Yuncheng Wu, Shaofeng Cai, Xiaokui Xiao, Gang Chen, and Beng Chin Ooi. Privacy preserving vertical federated learning for tree-based models. *arXiv preprint arXiv:2008.06170*, 2020.
- Xuefei Yin, Yanming Zhu, and Jiankun Hu. A comprehensive survey of privacy-preserving federated learning: A taxonomy, review, and future directions. *ACM Comput. Surv.*, 54(6), jul 2021. ISSN 0360-0300. doi:10.1145/3460427. URL <https://doi.org/10.1145/3460427>.
- Yang Liu, Yan Kang, Tianyuan Zou, Yanhong Pu, Yuanqin He, Xiaozhou Ye, Ye Ouyang, Ya-Qin Zhang, and Qiang Yang. Vertical federated learning, 2022a. URL <https://arxiv.org/abs/2211.12814>.
- Yang Liu, Yan Kang, Liping Li, Xinwei Zhang, Yong Cheng, Tianjian Chen, Mingyi Hong, and Qiang Yang. A communication efficient vertical federated learning framework. *Scanning Electron Microsc Meet at*, 2019.
- Qiang Yang, Yang Liu, Yong Cheng, Yan Kang, Tianjian Chen, and Han Yu. Federated learning. *Synthesis Lectures on Artificial Intelligence and Machine Learning*, 13(3):1–207, 2019.
- Fanglan Zheng, Kun Li, Jiang Tian, Xiaojia Xiang, et al. A vertical federated learning method for interpretable scorecard and its application in credit scoring. *arXiv preprint arXiv:2009.06218*, 2020.
- Liu Yang, Di Chai, Junxue Zhang, Yilun Jin, Leye Wang, Hao Liu, Han Tian, Qian Xu, and Kai Chen. A survey on vertical federated learning: From a layered perspective. *arXiv preprint arXiv:2304.01829*, 2023.
- Chong Fu, Xuhong Zhang, Shouling Ji, Jinyin Chen, Jingzheng Wu, Shanqing Guo, Jun Zhou, Alex X Liu, and Ting Wang. Label inference attacks against vertical federated learning. In *31st USENIX Security Symposium (USENIX Security 22)*, Boston, MA, 2022.
- Jiankai Sun, Xin Yang, Yuanshun Yao, and Chong Wang. Label leakage and protection from forward embedding in vertical federated learning. *arXiv preprint arXiv:2203.01451*, 2022.
- Oscar Li, Jiankai Sun, Xin Yang, Weihao Gao, Hongyi Zhang, Junyuan Xie, Virginia Smith, and Chong Wang. Label leakage and protection in two-party split learning. *arXiv preprint arXiv:2102.08504*, 2021.
- Eakalak Suthampan and Songrit Maneewongvatana. Privacy preserving decision tree in multi party environment. In Gary Geunbae Lee, Akio Yamada, Helen Meng, and Sung Hyon Myaeng, editors, *Information Retrieval Technology*, pages 727–732, Berlin, Heidelberg, 2005. Springer Berlin Heidelberg. ISBN 978-3-540-32001-2.
- Yang Liu, Yingting Liu, Zhijie Liu, Yuxuan Liang, Chuishi Meng, Junbo Zhang, and Yu Zheng. Federated forest. *IEEE Transactions on Big Data*, 2020.
- Jinpeng Hou, Mang Su, Anmin Fu, and Yan Yu. Verifiable privacy-preserving scheme based on vertical federated random forest. *IEEE Internet of Things Journal*, 2021.
- Fangcheng Fu, Yingxia Shao, Lele Yu, Jiawei Jiang, Huanran Xue, Yangyu Tao, and Bin Cui. Vf2boost: Very fast vertical federated gradient boosting for cross-enterprise learning. In *Proceedings of the 2021 International Conference on Management of Data, SIGMOD ’21*, page 563–576, New York, NY, USA, 2021. Association for Computing Machinery. ISBN 9781450383431. doi:10.1145/3448016.3457241. URL <https://doi-org.utokyo.idm.oclc.org/10.1145/3448016.3457241>.
- Weijing Chen, Guoqiang Ma, Tao Fan, Yan Kang, Qian Xu, and Qiang Yang. Secureboost+: A high performance gradient boosting tree framework for large scale vertical federated learning. *arXiv preprint arXiv:2110.10927*, 2021.
- Yang Xu, Xuexian Hu, Jianghong Wei, Hongjian Yang, and Kejia Li. Vf-cart: A communication-efficient vertical federated framework for the cart algorithm. *Journal of King Saud University - Computer and Information Sciences*, 35(1):237–249, 2023. ISSN 1319-1578. doi:<https://doi.org/10.1016/j.jksuci.2022.11.013>. URL <https://www.sciencedirect.com/science/article/pii/S1319157822004116>.

- Yang Liu, Zhuo Ma, Yilong Yang, Ximeng Liu, Jianfeng Ma, and Kui Ren. Revfrf: Enabling cross-domain random forest training with revocable federated learning. *IEEE Transactions on Dependable and Secure Computing*, 19(6): 3671–3685, 2022b. doi:10.1109/TDSC.2021.3104842.
- Houpu Yao, Jiazhou Wang, Peng Dai, Liefeng Bo, and Yanqing Chen. An efficient and robust system for vertically federated random forest. *arXiv preprint arXiv:2201.10761*, 2022.
- Zhihua Tian, Rui Zhang, Xiaoyang Hou, Jian Liu, and Kui Ren. Federboost: Private federated learning for gbdt. *arXiv preprint arXiv:2011.02796*, 2020.
- Hangyu Zhu, Rui Wang, Yaochu Jin, and Kaitai Liang. Pivodl: Privacy-preserving vertical federated learning over distributed labels. *IEEE Transactions on Artificial Intelligence*, 2021.
- Rui Wang, Oğuzhan Ersoy, Hangyu Zhu, Yaochu Jin, and Kaitai Liang. Feverless: Fast and secure vertical federated learning based on xgboost for decentralized labels. *IEEE Transactions on Big Data*, pages 1–15, 2022. doi:10.1109/TBDATA.2022.3227326.
- Tianqi Chen and Carlos Guestrin. Xgboost: A scalable tree boosting system. In *Proceedings of the 22nd acm sigkdd international conference on knowledge discovery and data mining*, pages 785–794, 2016.
- Vincent D Blondel, Jean-Loup Guillaume, Renaud Lambiotte, and Etienne Lefebvre. Fast unfolding of communities in large networks. *Journal of statistical mechanics: theory and experiment*, 2008(10):P10008, 2008.
- John A Hartigan and Manchek A Wong. Algorithm as 136: A k-means clustering algorithm. *Journal of the royal statistical society. series c (applied statistics)*, 28(1):100–108, 1979.
- Mohiuddin Ahmed, Raihan Seraj, and Syed Mohammed Shamsul Islam. The k-means algorithm: A comprehensive survey and performance evaluation. *Electronics*, 9(8):1295, 2020.
- Thomas M Cover. *Elements of information theory*. John Wiley & Sons, 1999.
- Qianying Liao, Bruno Cabral, João Paulo Fernandes, and Nuno Lourenço. Herb: Privacy-preserving random forest with partially homomorphic encryption. In *2022 International Joint Conference on Neural Networks (IJCNN)*, pages 1–10, 2022. doi:10.1109/IJCNN55064.2022.9892321.
- Pascal Paillier. Public-key cryptosystems based on composite degree residuosity classes. In *International conference on the theory and applications of cryptographic techniques*, pages 223–238. Springer, 1999.
- Dheeru Dua and Casey Graff. UCI machine learning repository, 2017. URL <http://archive.ics.uci.edu/ml>.
- Fabio Mendoza Palechor and Alexis de la Hoz Manotas. Dataset for estimation of obesity levels based on eating habits and physical condition in individuals from colombia, peru and mexico. *Data in brief*, 25:104344, 2019.
- C. De Stefano, M. Maniaci, F. Fontanella, and A. Scotto di Freca. Reliable writer identification in medieval manuscripts through page layout features: The “avila” bible case. *Eng. Appl. Artif. Intell.*, 72(C): 99–110, jun 2018. ISSN 0952-1976. doi:10.1016/j.engappai.2018.03.023. URL <https://doi.org/10.1016/j.engappai.2018.03.023>.
- Randal S. Olson, William La Cava, Patryk Orzechowski, Ryan J. Urbanowicz, and Jason H. Moore. Pmlb: a large benchmark suite for machine learning evaluation and comparison. *BioData Mining*, 10(1):36, Dec 2017. ISSN 1756-0381. doi:10.1186/s13040-017-0154-4. URL <https://doi.org/10.1186/s13040-017-0154-4>.
- Wallace Ugulino, Débora Cardador, Katia Vega, Eduardo Velloso, Ruy Milidiú, and Hugo Fuks. Wearable computing: Accelerometers’ data classification of body postures and movements. In *Advances in Artificial Intelligence-SBIA 2012: 21th Brazilian Symposium on Artificial Intelligence, Curitiba, Brazil, October 20-25, 2012. Proceedings*, pages 52–61. Springer, 2012.
- Alexander Kraskov, Harald Stögbauer, and Peter Grassberger. Estimating mutual information. *Physical review E*, 69(6): 066138, 2004.
- Andrew Rosenberg and Julia Hirschberg. V-measure: A conditional entropy-based external cluster evaluation measure. In *Proceedings of the 2007 joint conference on empirical methods in natural language processing and computational natural language learning (EMNLP-CoNLL)*, pages 410–420, 2007.
- Badih Ghazi, Noah Golowich, Ravi Kumar, Pasin Manurangsi, and Chiyuan Zhang. Deep learning with label differential privacy. *Advances in Neural Information Processing Systems*, 34:27131–27145, 2021.
- Wenliang Du and Zhijun Zhan. Building decision tree classifier on private data. In *Proceedings of the IEEE International Conference on Privacy, Security and Data Mining - Volume 14, CRPIT ’14*, page 1–8, AUS, 2002. Australian Computer Society, Inc. ISBN 0909925925.

- Jaideep Vaidya, Chris Clifton, Murat Kantarcioglu, and A Scott Patterson. Privacy-preserving decision trees over vertically partitioned data. *ACM Transactions on Knowledge Discovery from Data (TKDD)*, 2(3):1–27, 2008.
- Alka Gangrade and Ravindra Patel. Building privacy-preserving c4. 5 decision tree classifier on multi-parties. *International Journal on Computer Science and Engineering*, 1(3):199–205, 2009.
- Juntao Tan, Lan Zhang, Yang Liu, Anran Li, and Ye Wu. Residue-based label protection mechanisms in vertical logistic regression. *arXiv preprint arXiv:2205.04166*, 2022.
- Sanjay Kariyappa and Moinuddin K Qureshi. Gradient inversion attack: Leaking private labels in two-party split learning. *arXiv preprint arXiv:2112.01299*, 2021.
- Pengyu Qiu, Xuhong Zhang, Shouling Ji, Tianyu Du, Yuwen Pu, Jun Zhou, and Ting Wang. Your labels are selling you out: Relation leaks in vertical federated learning. *IEEE Transactions on Dependable and Secure Computing*, 2022.
- Aidmar Wainakh, Fabrizio Ventola, Till Müßig, Jens Keim, Carlos Garcia Cordero, Ephraim Zimmer, Tim Grube, Kristian Kersting, and Max Mühlhäuser. User-level label leakage from gradients in federated learning. *Proceedings on Privacy Enhancing Technologies*, 2022(2):227–244, 2022.
- Aidmar Wainakh, Till Müßig, Tim Grube, and Max Mühlhäuser. Label leakage from gradients in distributed machine learning. In *2021 IEEE 18th Annual Consumer Communications & Networking Conference (CCNC)*, pages 1–4, 2021. doi:10.1109/CCNC49032.2021.9369498.
- Sebastiaan de Hoogh, Berry Schoenmakers, Ping Chen, et al. Practical secure decision tree learning in a telemedicine application. In *International Conference on Financial Cryptography and Data Security*, pages 179–194. Springer, 2014.
- Samuel Adams, Chaitali Choudhary, Martine De Cock, Rafael Dowsley, David Melanson, Anderson CA Nascimento, Davis Railsback, and Jianwei Shen. Privacy-preserving training of tree ensembles over continuous data. *arXiv preprint arXiv:2106.02769*, 2021.
- Mark Abspoel, Daniel Escudero, and Nikolaj Volgushev. Secure training of decision trees with continuous attributes. Cryptology ePrint Archive, Paper 2020/1130, 2020. URL <https://eprint.iacr.org/2020/1130>. <https://eprint.iacr.org/2020/1130>.
- Kevin Deforth, Marc Desgroseilliers, Nicolas Gama, Mariya Georgieva, Dimitar Jetchev, and Marius Vuille. Xorboost: Tree boosting in the multiparty computation setting. *Cryptology ePrint Archive*, 2021.
- Wenjing Fang, Derun Zhao, Jin Tan, Chaochao Chen, Chaofan Yu, Li Wang, Lei Wang, Jun Zhou, and Benyu Zhang. Large-scale secure xgb for vertical federated learning. In *Proceedings of the 30th ACM International Conference on Information & Knowledge Management*, pages 443–452, 2021.
- Cynthia Dwork, Aaron Roth, et al. The algorithmic foundations of differential privacy. *Foundations and Trends® in Theoretical Computer Science*, 9(3–4):211–407, 2014.
- Mário S Alvim, Miguel E Andrés, Konstantinos Chatzikokolakis, Pierpaolo Degano, and Catuscia Palamidessi. Differential privacy: on the trade-off between utility and information leakage. In *International Workshop on Formal Aspects in Security and Trust*, pages 39–54. Springer, 2011.
- Amos Beimel, Kobbi Nissim, and Uri Stemmer. Private learning and sanitization: Pure vs. approximate differential privacy. In *Approximation, Randomization, and Combinatorial Optimization. Algorithms and Techniques*, pages 363–378. Springer, 2013.
- Kamalika Chaudhuri and Daniel Hsu. Sample complexity bounds for differentially private learning. In Sham M. Kakade and Ulrike von Luxburg, editors, *Proceedings of the 24th Annual Conference on Learning Theory*, volume 19 of *Proceedings of Machine Learning Research*, pages 155–186, Budapest, Hungary, 09–11 Jun 2011. PMLR. URL <https://proceedings.mlr.press/v19/chaudhuri11a.html>.
- Tianhao Wang, Yuheng Zhang, and Ruoxi Jia. Improving robustness to model inversion attacks via mutual information regularization. In *Proceedings of the AAAI Conference on Artificial Intelligence*, volume 35, pages 11666–11673, 2021.
- Farhad Farokhi and Mohamed Ali Kaafar. Modelling and quantifying membership information leakage in machine learning. *arXiv preprint arXiv:2001.10648*, 2020.
- Stanley L Warner. Randomized response: A survey technique for eliminating evasive answer bias. *Journal of the American Statistical Association*, 60(309):63–69, 1965.

A Tree-based Vertical Federated Learning (T-VFL) algorithms

Algorithms 3 and 4 depict the typical workflows to construct a tree in Tree-based Vertical Federated Learning (T-VFL) for the passive and active parties, respectively. Since each T-VFL protocol mentioned in Sections 1 and 6 adopts different methods, we provide only abstract overviews here. In T-VFL, the passive party (\mathcal{P}_m) usually receives the instance space of a node to be divided (\mathbb{D}). Then, the passive party iterates through all features (ϕ) and calculates the percentiles of each feature on the instances in \mathbb{D} . Next, the passive party generates a binary split for each feature by comparing each instance's feature value to the selected percentile. The split is evaluated using a scoring function, and the result is stored in Γ^m . As the scoring function, Random Forest typically uses gini impurity for classification, and XGBoost adopts its own gain function. Once all splits for all features are evaluated, Γ^m is sent to the active party (\mathcal{P}_1). If \mathcal{P}_m is chosen as the best party, it receives the best-split index k^* from \mathcal{P}_1 and sends the instance spaces of the two child nodes generated by the best split to \mathcal{P}_1 . These procedures are recursively continued until termination conditions, such as depth constraints, are met.

Algorithm 3 Split Finding for T-VFL (Passive Party)

```

1:  $\mathcal{P}_m$  receives the instance space  $\mathbb{D}$  of a node to be divided
2:  $\Gamma^m \leftarrow \{\}$ 
3: for  $\phi = 1 \leftarrow |\mathbb{F}_m|$  do
4:    $\{s_{\phi,1}, s_{\phi,2}, \dots, s_{\phi,l}\} \leftarrow \text{percentiles on } \{x_{i,\phi}^m \mid i \in \mathbb{D}\}$ 
5:   for  $v = 1$  to  $l$  do
6:     Left instance space by this split  $\leftarrow \{i \mid i \in \mathbb{D}, x_{i,\phi}^m < s_{\phi,l}\}$ 
7:     Right instance space by this split  $\leftarrow \{i \mid i \in \mathbb{D}, x_{i,\phi}^m \geq s_{\phi,l}\}$ 
8:     Add the evaluation of this split to  $\Gamma^m$ 
9:  $\mathcal{P}_m$  sends  $\Gamma^m = \{\sigma_{m,k}\}$ , the evaluation for each split candidate, to  $\mathcal{P}_1$ 
10: if  $\mathcal{P}_m$  is selected as the best party then
11:    $\mathcal{P}_m$  receives  $k^*$  from  $\mathcal{P}_1$ 
12:    $\mathcal{P}_m$  sends the instance spaces of the children nodes generated by  $k^*$ 

```

Algorithm 4 Split Finding for T-VFL (Active Party)

```

1:  $\mathcal{P}_1$  broadcasts the instance space  $\mathbb{D}$  of a node to be divided
2:  $\mathcal{P}_1$  gathers the evaluation of split candidates  $\Gamma = \{\Gamma^m\}_{m=1}^M$ .
3:  $\mathcal{P}_1$  picks the best split  $\sigma_{m^*,k^*}$  from  $\Gamma$ .
4:  $\mathcal{P}_1$  notify  $k^*$  to  $\mathcal{P}_{m^*}$ 
5:  $\mathcal{P}_1$  receives the instance space of children nodes from  $\mathcal{P}_{m^*}$ 
6: If terminated conditions are not satisfied, the children are recursively trained.

```

B Adjacency Matrix

Algo. 5 is the pseudocode algorithm for creating a memory-efficient adjacency matrix. If the size of the instance space is greater than or equal to the chunk size B , the algorithm adds inter-chunk edges with a weight of w' between the end of one chunk and the beginning of the next. It then iterates through all pairs of the instance space within each chunk and adds the same edge with a weight of η^{t-1} to the adjacency matrix.

Algorithm 5 Memory Efficient Adjacency Matrix for Community Detection

Require: Adjacency matrix A , the instance space $\mathbb{D}_u^t = \{i_1, i_2, \dots, i_{|\mathbb{D}_u^t|}\}$, the chunk size B , the discount factor η and weight of inter-chunk edge w'

- 1: **if** u -th node within t -th tree is not a leaf **then return**
- 2: **if** $|\mathbb{D}_u^t| < B$ **then**
- 3: **for** $j \leftarrow 1$ to $|\mathbb{D}_u^t|$ **do**
- 4: **for** $k \leftarrow j + 1$ to $|\mathbb{D}_u^t|$ **do**
- 5: $A_{i_j, i_k} \leftarrow A_{i_j, i_k} + \eta^{t-1}$
- 6: $A_{i_k, i_j} \leftarrow A_{i_k, i_j} + \eta^{t-1}$ ▷ Add intra-chunk edges
- 7: **else**
- 8: $s \leftarrow 0, \quad t \leftarrow 0$
- 9: **while** $s \leq |\mathbb{D}_u^t|$ **do**
- 10: **if** $s \neq 0$ **then**
- 11: $A_{i_s, i_t} \leftarrow A_{i_s, i_t} + w'$
- 12: $A_{i_t, i_s} \leftarrow A_{i_t, i_s} + w'$ ▷ Add an inter-chunk edge
- 13: $t \leftarrow \min(s + B, |\mathbb{D}_u^t| + 1)$
- 14: **for** $j \leftarrow s$ to $t - 1$ **do**
- 15: **for** $k = j + 1$ to $t - 1$ **do**
- 16: $A_{i_j, i_k} \leftarrow A_{i_j, i_k} + \eta^{t-1}$
- 17: $A_{i_k, i_j} \leftarrow A_{i_k, i_j} + \eta^{t-1}$ ▷ Add intra-chunk edges
- 18: $s \leftarrow t$

C Louvain Method

Louvain method [Blondel et al., 2008] is one of the popular community detection methods that groups vertices of a graph G into a set of communities com . Let \mathbb{V} be the set of vertices of graph G . We denote the partition of the vertices as $\mathbb{P} = \bigcup_{\pi} \mathbb{P}_{\pi}$, where \mathbb{P}_{π} is the π -th community of G ; $\mathbb{P}_{\pi} \subseteq \mathbb{V}$. As described in (3,2), Louvain method (Algo. 6) mainly consists of two steps; moving vertices (Algo. 7), and aggregation (Algo. 8). First, Louvain method makes each vertex a unique community; $\forall v \in \mathbb{V} \quad \mathbb{P}_v \leftarrow \{v\}$, and $\mathbb{P} = \bigcup_v \mathbb{P}_v$. In the moving vertices phase, Louvain method repeatedly picks one random vertex and changes its community to the best neighboring community that maximizes modularity (Eq. 4). When the modularity cannot be optimized anymore, Louvain method aggregates the vertices by their communities and creates a new graph. Specifically, the vertices of the updated graph are the communities of the previous graph. The edge weight between two vertices of the updated graph is the sum of edge weights that connects the corresponding two communities of the previous graph. Note that Louvain method uses the sum of edge weights within a community of the previous graph as the self-loop edge of the corresponding vertex of the new graph.

Algorithm 6 Louvain

Require: Graph G
Ensure: Set of communities com

- 1: $\mathbb{V}^{(0)} \leftarrow$ initial set of vertices of G
- 2: $\mathbb{V} \leftarrow \mathbb{V}^{(0)}$
- 3: $\forall v \in \mathbb{V} \quad \mathbb{P}_v \leftarrow \{v\}, \quad \mathbb{P} = \bigcup_v \mathbb{P}_v$ ▷ initial partition
- 4: **while do**
- 5: $\mathbb{P} \leftarrow \text{MoveVertices}(G, \mathbb{P})$ ▷ Algo. 7
- 6: **if** $|\mathbb{V}| \neq |\mathbb{P}|$ **then**
- 7: **Break**
- 8: $G, \mathbb{V}' \leftarrow \text{Aggregate}(G, \mathbb{P})$ ▷ Algo. 8
- 9: $\forall v \in \mathbb{V} \quad \mathbb{P}_v \leftarrow \{v\}, \quad \mathbb{P} = \bigcup_v \mathbb{P}_v$
- 10: $\text{com} \leftarrow$ convert \mathbb{P} to the final partition of each vertex of $\mathbb{V}^{(0)}$ from the correspondence between $\mathbb{V}^{(0)}$ and \mathbb{V}
- 11: **return** com

Algorithm 7 MoveVertices

Require: Graph G
Ensure: Updated partition \mathbb{P}

- 1: **while** $Q(G, \mathbb{P}) >$ previous Q **do**
- 2: **for** randomly pick $v \in \mathbb{V}$ **do**
- 3: $\pi \leftarrow$ index of current community of v
- 4: $\pi^* \leftarrow \text{SelectCommunity}(v)$
- 5: $\mathbb{P}_{\pi} = \mathbb{P}_{\pi} \setminus \{v\}, \mathbb{P}_{\pi^*} = \mathbb{P}_{\pi^*} \cup \{v\}$
- return** \mathbb{P}

Algorithm 8 Aggregate**Require:** Graph G , partition \mathbb{I} **Ensure:** Aggregated graph G'

- 1: $\mathbb{V} \leftarrow$ set of vertices of G
- 2: $A \in \mathbb{R}^{|\mathbb{V}| \times |\mathbb{V}|} \leftarrow$ adjacency matrix of G
- 3: Generate new matrix $A' \in \mathbb{R}^{|\mathbb{I}| \times |\mathbb{I}|}$
- 4: **for** $\pi, \pi' = 1, \dots, |\mathbb{I}|$ **do**
- 5: $A'_{\pi, \pi'} = \sum_{v, v'} A_{v, v'} \mathbb{1}(v \in \mathbb{I}_\pi) \mathbb{1}(v' \in \mathbb{I}_{\pi'})$
- return** $G', \mathbb{V}' \leftarrow$ convert A' to a new graph

Algorithm 9 SelectCommunity**Require:** vertex v , greed parameter θ **Ensure:** the index of best community

- 1: **for** $\pi \leftarrow$ neighboring communities of v **do**
- 2: **if** moving v to π improves Q **then**
- 3: Assign π to v
- return** The index of community of v

D K-Means

Given the specified cluster numbers K , K-means [Hartigan and Wong, 1979] groups the dataset into K clusters. As in Algo. 10, K-means first randomly create K centroids. Then, K-means iteratively assigns the closest cluster to each data point and updates the centroids.

Algorithm 10 K-Means**Require:** Training dataset D , the number of clusters K

- 1: Generate K random data points as initial centroids.
- 2: **while** Convergence conditions not met **do**
- 3: **for** each data point of the dataset D **do**
- 4: $k^* \leftarrow$ the index of closed centroids
- 5: Assign k^* to this data point
- 6: each centroid \leftarrow the mean of assigned data points.

E Proofs of ID-LMID

Proof of Theorem 1. Since by definition $I(Y; S_w) = E_{S_w}[D_{KL}(P(Y|S_w) || P(Y))]$, where D_{KL} is KL-Divergence, and E is expected value, we have the upper bound as follows:

$$\begin{aligned}
I(Y; S_w) &= E_{S_w}[D_{KL}(P(Y|S_w) || P(Y))] \\
&\leq \max_{s \in \{0,1\}} (D_{KL}(P(Y|S_w = s) || P(Y))) \\
&= \max_{s \in \{0,1\}} \left(\sum_{c \in \mathbb{C}} P_{Y|S_w=s}(c) \log \frac{P_{Y|S_w=s}(c)}{P_Y(c)} \right)
\end{aligned} \tag{6}$$

Recall that S_w is 1 when the data belongs to the node, and 0 otherwise. Since $P(Y)$ is the label distribution, $P(Y|S_w = 1)$, and $P(Y|S_w = 0)$ are the label distribution within the w -th node and outside the w -th node, respectively, we can empirically approximate these terms as follows:

$$P_Y(c) = N_c/N, \quad P_{Y|S_w=1}(c) = n_c^w/n^w, \quad P_{Y|S_w=0}(c) = \bar{n}_c^w/\bar{n}^w \tag{7}$$

Combining Eq. 6 and Eq. 7 yields Eq. 3. □

Proof of Proposition 1. Let H denote the entropy function. Then, we have the following:

$$I(Y; S_1, S_2, \dots, S_w, \dots, S_W) \quad (8)$$

$$= \sum_{w=1}^W [H(S_w; S_1, S_2, \dots, S_{w-1}) - H(S_w; Y, S_1, S_2, \dots, S_{w-1})] \quad (9)$$

$$\leq \sum_{w=1}^W [H(S_w) - H(S_w; Y, S_1, S_2, \dots, S_{w-1})] \quad (10)$$

$$= \sum_{w=1}^W [H(S_w) - H(S_w; Y)] + \sum_{w=1}^W [H(S_w; Y) - H(S_w; Y, S_1, S_2, \dots, S_{w-1})] \quad (11)$$

$$= \sum_{w=1}^W I(Y; S_w) + \sum_{w=1}^W [H(S_w; Y) - H(S_w; Y, S_1, S_2, \dots, S_{w-1})] \quad (12)$$

$$\leq W\xi + (W - 1) \log 2 \quad (13)$$

We use the fact that conditioning reduces entropy in Eq. 10, and S_w is 0 or 1, which makes the maximum value of $H(S_w)$ be $\log 2$ in Eq. 13. \square

F V-measure

Rosenberg and Hirschberg [2007] proposes V-measure, which is the average of Homogeneity and Completeness. First, we denote the entropy of class distribution, that of cluster distribution, the conditional entropy of class distribution given the clustering, and its opposite as $H(\mathbb{C})$, $H(\mathbb{K})$, $H(\mathbb{C}|\mathbb{K})$, and $H(\mathbb{K}|\mathbb{C})$ respectively. Then, V-measure calculates them as follows:

$$\begin{aligned} H(\mathbb{C}|\mathbb{K}) &= - \sum_{k \in \mathbb{K}} \sum_{c \in \mathbb{C}} \frac{n_{c,k}}{N} \log \frac{n_{c,k}}{\sum_{c \in \mathbb{C}} n_{c,k}} & H(\mathbb{C}) &= - \sum_{c \in \mathbb{C}} \frac{\sum_{k \in \mathbb{K}} n_{c,k}}{N} \log \frac{\sum_{k \in \mathbb{K}} n_{c,k}}{N} \\ H(\mathbb{K}|\mathbb{C}) &= - \sum_{c \in \mathbb{C}} \sum_{k \in \mathbb{K}} \frac{n_{c,k}}{N} \log \frac{n_{c,k}}{\sum_{k \in \mathbb{K}} n_{c,k}} & H(\mathbb{K}) &= - \sum_{k \in \mathbb{K}} \frac{\sum_{c \in \mathbb{C}} n_{c,k}}{N} \log \frac{\sum_{c \in \mathbb{C}} n_{c,k}}{N} \end{aligned}$$

Homogeneity quantifies the similarities of the samples in a cluster as the following:

$$\text{Homogeneity} = \begin{cases} 1 & \text{if } H(\mathbb{C}) = 0 \\ 1 - \frac{H(\mathbb{C}|\mathbb{K})}{H(\mathbb{C})} & \text{otherwise} \end{cases} \quad (14)$$

On the other hand, Completeness measures how much data belonging to a label is assigned to the same cluster as follows:

$$\text{Completeness} = \begin{cases} 1 & \text{if } H(\mathbb{K}) = 0 \\ 1 - \frac{H(\mathbb{K}|\mathbb{C})}{H(\mathbb{K})} & \text{otherwise} \end{cases} \quad (15)$$

Then, V-measure is defined with the following equation:

$$V = \frac{2 * \text{Homogeneity} * \text{Completeness}}{\text{Homogeneity} + \text{Completeness}} \quad (16)$$

G LP-MST

LP-MST [Ghazi et al., 2021] enables training a label differentially private model based on PRWithPrior algorithm (Algo. 11), which privately randomizes each label of the dataset while minimizing the injected noise. PRWithPrior determines the best threshold c^* given the prior distribution and applies the randomized response [Warner, 1965] if the corresponding probability of the input label is within the top c^* of the prior distribution. If not, PRWithPrior returns

the uniformly random label. To get good prior distribution for each label privately, LP-MST (Algo. 12) first splits the dataset D into T disjoint subsets; $D = \bigcup_{t=1}^T D^{(t)}$. We denote a model that always assigns an equal probability for each class as $\mathcal{M}^{(0)}$. Then, LP-MST randomizes each label of $D^{(t)}$ with PRWithPrior, using the prediction of $\mathcal{M}^{(t)}$ as the prior distribution for each data point. After randomizing labels, LP-MST trains t -th model on the randomized datasets $\bigcup_{t'=1}^{t-1} \tilde{D}^{(t')}$. For implementation and communication simplicity, we train all $\mathcal{M}^{(t)}$, $t = 1, \dots, T - 1$ with only the active party and trains the final $\mathcal{M}^{(T)}$ with all parties.

Algorithm 11 RRWithPrior

Require: A label $y \in \mathbb{C}$, prior distribution $\{p_c\}_{c \in \mathbb{C}}$, privacy budget ϵ
Ensure: A randomized label y'

- 1: **for** $c \in \mathbb{C}$ **do**
- 2: $\mathbb{Y}_c \leftarrow$ the set of labels with top c prior probabilities.
- 3: $w_c = \frac{e^\epsilon}{e^\epsilon + c - 1} (\sum_{\hat{y} \in \mathbb{C}} p_{\hat{y}})$
- 4: $c^* = \arg \max_c w_c$
- 5: **if** $y \in \mathbb{Y}_{c^*}$ **then**
- 6: $\begin{cases} y' = y & w.p. \frac{e^\epsilon}{e^\epsilon + c^* - 1} \\ y' \in \mathbb{Y}_{c^*} \setminus \{y\} & w.p. \frac{1}{e^\epsilon + c^* - 1} \end{cases}$
- 7: **else**
- 8: $y' \leftarrow$ uniformly random element of \mathbb{Y}_{c^*}
- return** y'

Algorithm 12 LP-MST

Require: Training dataset $D = \{(x_1, y_1), \dots, (x_N, y_N)\}$, training algorithm \mathcal{A} , number of stages T , privacy budget ϵ
Ensure: Trained model that satisfies ϵ -LDP

- 1: Let $\mathcal{M}^{(0)}$ assign the same probability to each class for any input.
- 2: Divide D into subsets $D^{(1)}, \dots, D^{(T)}$
- 3: **for** $t = 1, \dots, T$ **do**
- 4: $\tilde{D}^{(t)} = \emptyset$
- 5: **for** $(x_i, y_i) \in D^{(t)}$ **do**
- 6: $\{p_c\}_{c \in \mathbb{C}} \leftarrow$ prediction of $\mathcal{M}^{(t-1)}$ on x_i
- 7: $\tilde{y}_i = \text{PRWithPrior}(y_i, \{p_c\}_{c \in \mathbb{C}}, \epsilon)$
- 8: $\tilde{D}^{(t)} = \tilde{D}^{(t)} \cup \{x_i, \tilde{y}_i\}$
- 9: $\mathcal{M}^{(t)} = \mathcal{A}(\bigcup_{t'=1}^t \tilde{D}^{(t')})$
- return** $\mathcal{M}^{(T)}$

H Experiments

Tab. 2 shows the details of each dataset. We use the memory-efficient adjacency matrix for *Drive*, *Fars*, and *Pucrio* with a chunk size of 1000 and inter-chunk weight of 100.

Table 2: Statistics of Datasets

Dataset	Number of Samples	Number of Features	Number of Classes
<i>Breastcancer</i>	569	30	2
<i>Obesity</i>	2111	17	7
<i>Phishing</i>	11055	30	2
<i>Nursery</i>	12960	8	5
<i>Credit</i>	30000	24	2
<i>Avila</i>	20867	10	12
<i>Drive</i>	58509	49	11
<i>Fars</i>	100968	30	8
<i>Pucrio</i>	165632	18	5

Visualization of Clustering Fig. 7 visualizes the clusters of ID2Graph and CL extracted from Random Forest on *Breastcancer* and *Phishing*. We reduce the dimension of features to 2 with PCA before applying it to K-means for visualization. All other parameter settings are the same. It shows that ID2Graph results in more accurate clustering than CL.

Impact of Tree Depth. The performance of ID2Graph is also impacted by the maximum depth constraint of the tree model, as shown in Fig. 8. Increasing the depth generally leads to more label leakage in ID2Graph. Still, it's worth noting that going too deep can sometimes worsen attack results. As the depth of the tree increases, the instance space at the leaves becomes purer but smaller. In other words, fewer classes and samples are assigned in the instance space as the tree splits. ID2Graph relies on the assumption that the data samples within the instance space have similar class

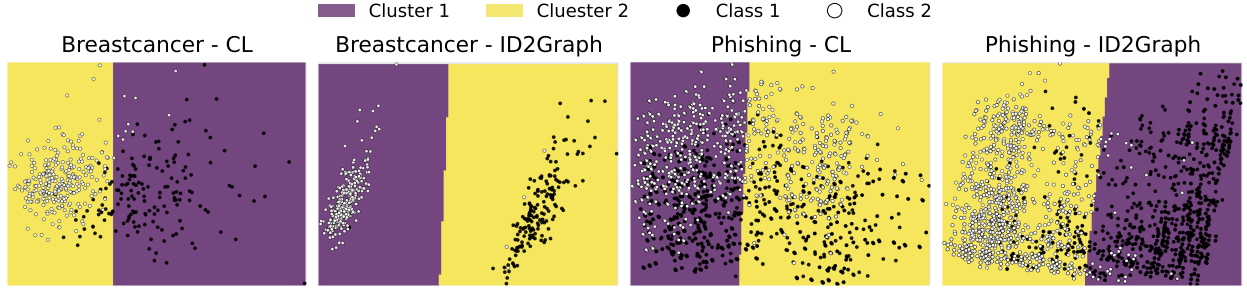


Figure 7: Example of obtained clusters on *Breastcancer* and *Phishing*. The marker color corresponds to the binary class label, and the background color shows the region of each cluster. The clusters extracted with ID2Graph are more correlated to the ground-truth labels.

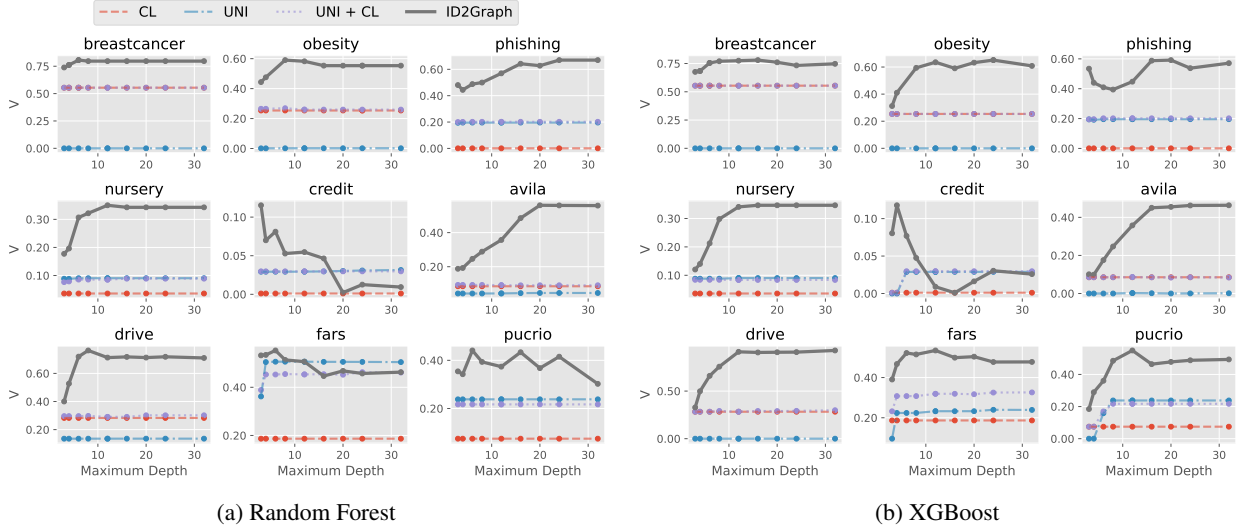


Figure 8: Impact of tree depth on attack performance. Deeper depth improves the attack performance of ID2Graph in many cases, but too deep depth can be harmful in some cases.

labels. While fewer classes can be beneficial, having too small of an instance space can be detrimental. Extremely, if all the leaves contain only one sample, it is impossible to extract useful relationship information from leaves.

Impact of Number of Trees We also investigate the impact of the number of trees on attack performance. As shown in Fig. 9, ID2Graph outperforms other baselines in most settings. Fig. 9 also reveals that while increasing the number of trees generally improves the attack performance, too many trees decrease attack performance, especially when attacking XGBoost. This is compatible with a prior work [Cheng et al., 2021], which finds that the latter trees in the forest have relatively less information about training labels. We also find that UNI does not work, especially for the cases with more giant forests, since all samples are unified into one cluster.

Impact of Feature Partition. The performance of ID-LMID also depends on the availability of features at the active party since ID-LMID replaces all split candidates received from passive parties that do not meet Eq. 4 with children trained exclusively with data at the active party. Fig. 10 shows the results when the active party has no features, while all other settings are kept the same as Fig. 4. Reduced-Leakage defense is not applicable in this scenario, and the number of stages of LP-MST is 1. While the AUC of ID-LMID with the same ξ is generally lower compared to Fig. 4, ID-LMID still achieves better utility-privacy tradeoffs than LP-MST.

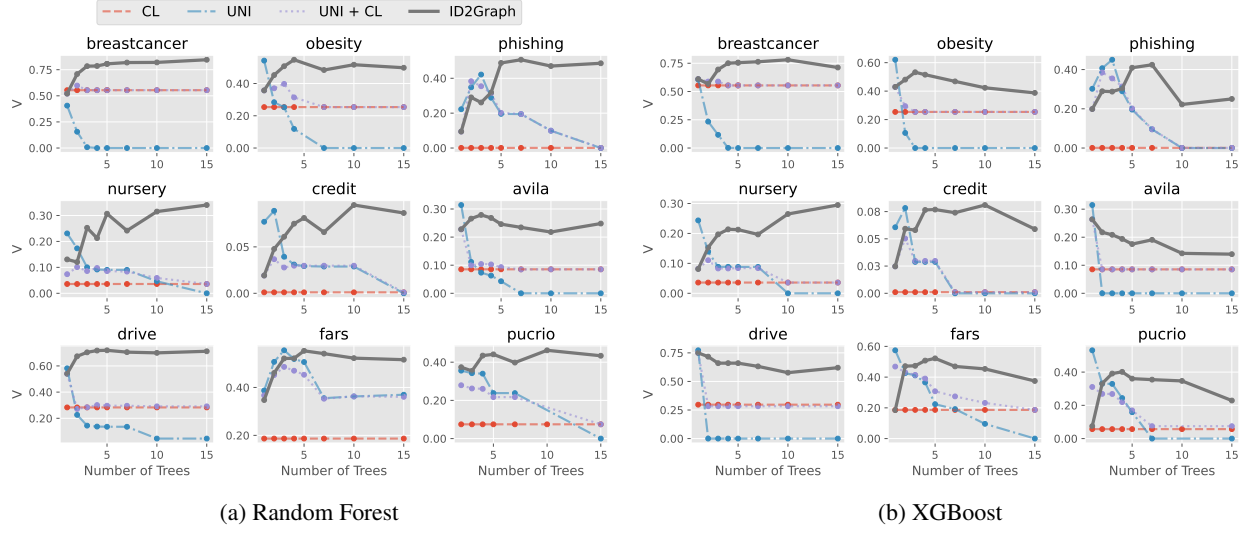


Figure 9: Impact of the number of trees.

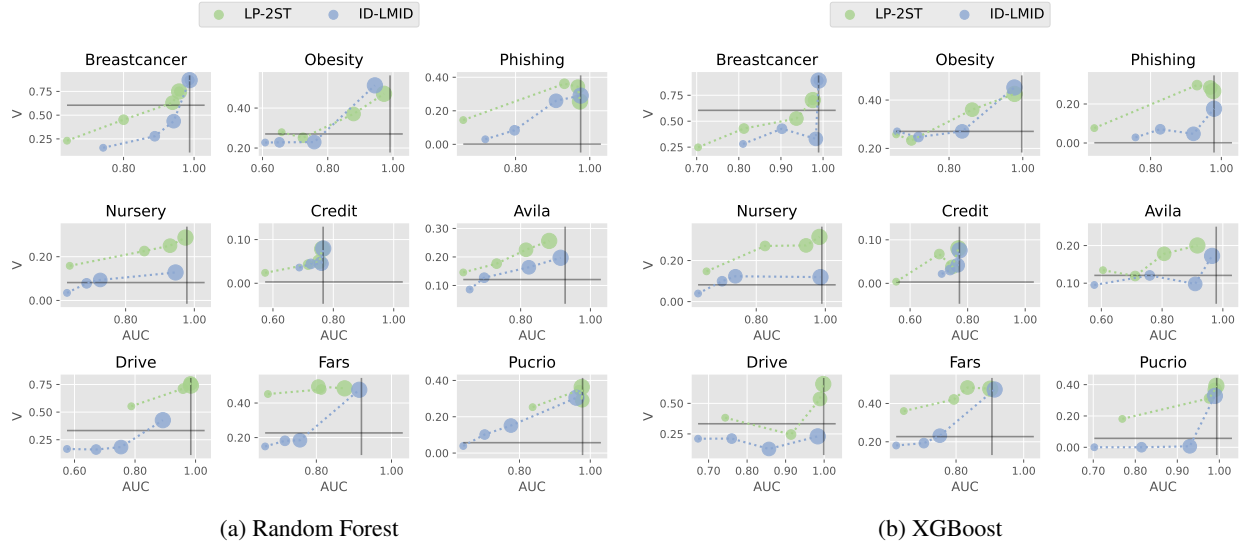


Figure 10: Defense results against ID2Graph when the active party does not have any features. ID2Graph still outperforms other methods in most cases.